



Nucleate and convective boiling in plate fin heat exchangers

A. Feldman^a, C. Marvillet^b, M. Lebouché^{c,*}

^a*ProFroid Industries, 178, rue du Fauge ZI des Paluds, BP 1152, 13782 Aubagne Cedex, France*

^b*CEA-Grenoble/DRN/DTP/Groupement Ademe/CEA pour la Recherche sur les Echangeurs Thermiques, 17, rue de Martyrs, 38054 Grenoble Cedex 9, France*

^c*Laboratoire d'Energétique et de Mécanique Théorique et Appliquée (LEMETA), CNRS URA 875 Université H. Poincaré, 2, avenue de la Forêt de Haye, BP 160, 54504 Vandoeuvre Cedex, France*

Received 5 November 1996; received in revised form 7 June 1999

Abstract

The results of laboratory experiments with CFC114 flowing in an electrically heated, serrated-fin or perforated fin test section to measure local boiling coefficients over a wide range of vapour quality, with mass fluxes up to 45 kg/m² s, heat fluxes up to 3500 W/m² and pressure of 3 bar are reported. These low mass and heat fluxes reflect the industrial process application of these heat exchangers where small temperature differences may exist between streams.

An analysis of the measured heat transfer coefficients from tests with CFC114 in both serrated fin and perforated fin geometries shows the separate effects of quality, mass flux and heat flux.

Two kinds of mechanism were found: a nucleate boiling regime and a convective boiling regime. The data were predicted using an asymptotic model, the nucleate boiling component was obtained from pool boiling data and the forced convective component of the two-phase heat transfer coefficient was found to be well represented by the *F* and Martinelli parameters used by Chen [I&EC Process Design and Development 5(3) (1966)]. © 2000 Elsevier Science Ltd. All rights reserved.

1. Introduction

Finned flow passage geometries have been widely used in single-phase compact heat exchanger applications. Over the past decade, compact heat exchanger surfaces have been used more and more widely in applications involving phase changes, such as cryogenic processing system for liquefaction of natural gas, hydrocarbon separation and automotive air-conditioning.

Aluminium plate fin heat exchangers also offer process integration possibilities (12 or more simultaneous streams in one exchanger), and high energy efficiency under a tight temperature approach (1 or 2°C) in a large variety of geometries.

The design of this type of heat exchanger may be largely influenced by two important features: first, the fin geometry which may be of 'offset strip' fin or 'perforated' type; secondly, the hydraulic diameter which can be very small (about 1 mm for the tested geometries presented in this report) and which greatly depends on fin geometrical parameter (fin height and pitch). These heat exchangers are

* Corresponding author. Tel.: +33-03-83-59-56-08; fax: +33-03-83-59-55-44.

Nomenclature

A	area (m ²)		
C_p	specific heat at constant pressure (J/kg K)		
D_h	hydraulic diameter (m)		
F	enhancement factor		
h	fin height (m)		
h_{fg}	latent heat of vaporization (J/kg)		
L	fin length (m)		
\dot{m}	mass flow velocity (kg/m ² s)		
\dot{M}	mass flow rate (kg/s)		
\tilde{M}	molecular weight (kg/mol)		
n	exposant in the asymptotic model		
N	number of fins		
p	pressure (bar)		
p_{red}	reduced pressure (bar)		
\dot{q}	heat flux (W/m ²)		
\dot{Q}	power (W)		
T	temperature (°C)		
x	vapour quality		
X	Lockhart–Martinelli parameter		
		<i>Greek symbols</i>	
		α	heat transfer coefficient (W/m ² K)
		δ	fin thickness (m)
		Δ	difference
		<i>Subscripts</i>	
		cv	convective boiling
		g	vapour
		in	inlet
		l	liquid
		l	laminar
		nb	nucleate boiling
		npb	nucleate pool boiling
		out	outlet
		sat	saturation
		t	turbulent
		tp	two-phase
		w	wall

currently used in many processes as an evaporator in a thermosyphon loop. To avoid excessive pressure drop of the evaporating fluid, mass flux in the finned passage is kept at low values (in this study $20 < \dot{m} < 45 \text{ kg m}^{-2} \text{ s}^{-1}$).

Some authors have already worked on boiling in compact heat exchangers. Experimental results have been obtained by Robertson [1] and Robertson and Lovegrove [2] with nitrogen and CFC11. Robertson [3,4] also developed two different models for predicting local heat transfer coefficients for annular flow in these geometries.

In more recent studies, Carey and Mandrusiak [5–7] examined the effects of channel geometry on the local heat transfer coefficient for flow boiling, visualised the flow in the channel and proposed an expression for computing the two-phase heat transfer coefficient.

The GRETh (Groupement pour la Recherche sur les Echangeurs Thermiques) has been engaged in research into this type of exchanger for a number of years in single phase applications [8,9]. The need to understand the performance characteristics of these configurations used for phase change has led the GRETh to carry out a study to obtain direct visual observations, the local heat transfer coefficient and the local pressure law.

The proposed paper presents local boiling heat transfer data in plate fin passages. Tests were carried out under saturated conditions at 36°C with CFC114

and two kinds of fin: offset strip fins and perforated fins, whose dimensions are given in Table 1.

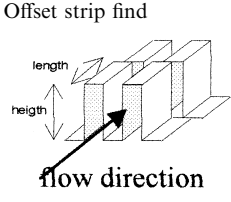
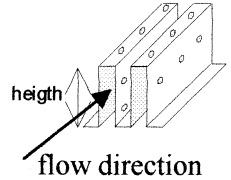
The present study was undertaken to achieve two main objectives. The primary objective was to obtain local heat transfer coefficients during flow boiling and to quantify the contribution of nucleate boiling or convective boiling to the heat transfer coefficient. The secondary objective was to study the influence of the fin geometrical parameters over the heat transfer coefficients and to propose a method for predicting the heat transfer coefficient, regardless of the fin geometry.

2. Experimental apparatus

The experimental apparatus (Fig. 1) allowed boiling in plate-fin heat exchangers to be studied during an ascendant flow of pure refrigerant. It consisted of three circuits: a cold water, a hot water and a refrigerant circuit.

The test section was inserted in the main circuit which provided a steady flow of pure refrigerant: liquid flow from the reservoir to the preheater was provided by a variable speed circulation pump and a mass flow rate transmitter (Coriolis type) measured the mass flow rate. The preheater evaporated some of the refrigerant using the hot water circuit to provide a two-phase flow through the section. The preheater power input was controlled to adjust the inlet quality to the test section. After the fluid passed through the test section it was

Table 1
Dimensions of the fins

		Offset strip find	Perforated fins
			
		OSF01/OSF02	Perf01/Perf02/Perf03
Fin height	h (mm)	6.93/6.93	6.93/3.33/6.93
Fin length	L (mm)	3.18/9.52	
Fin thickness	δ (mm)	0.2/0.2	0.2/0.2/0.2
Fins per inch	N	18/22	18/18/25
Hydraulic diameter	D_h (mm)	2.06/1.98	2.06/1.78/1.67

condensed back to subcooled liquid in a water cooled condenser. With this test loop, experimental data were obtained for vapour qualities ranging from 5 to 80% and mass flux values ranging from 20 to 45 kg/m² s.

Each test section consisted of a single channel with fins between two aluminium slabs, 400 mm long and 150 mm wide (Fig. 2). Adhesive resistances (230 V, 1300 W) heated the slabs; thus, heat

was conducted through the slabs to the finned surface where it was transferred to the fluid flowing in the channel. Available heat flux values ranged from 1000 to 3500 W/m². Eight thermocouples were also embedded in the slab as shown in Fig. 3 to measure the wall temperature.

Determination of the wall temperature is necessary for calculation of the local heat transfer coefficient.

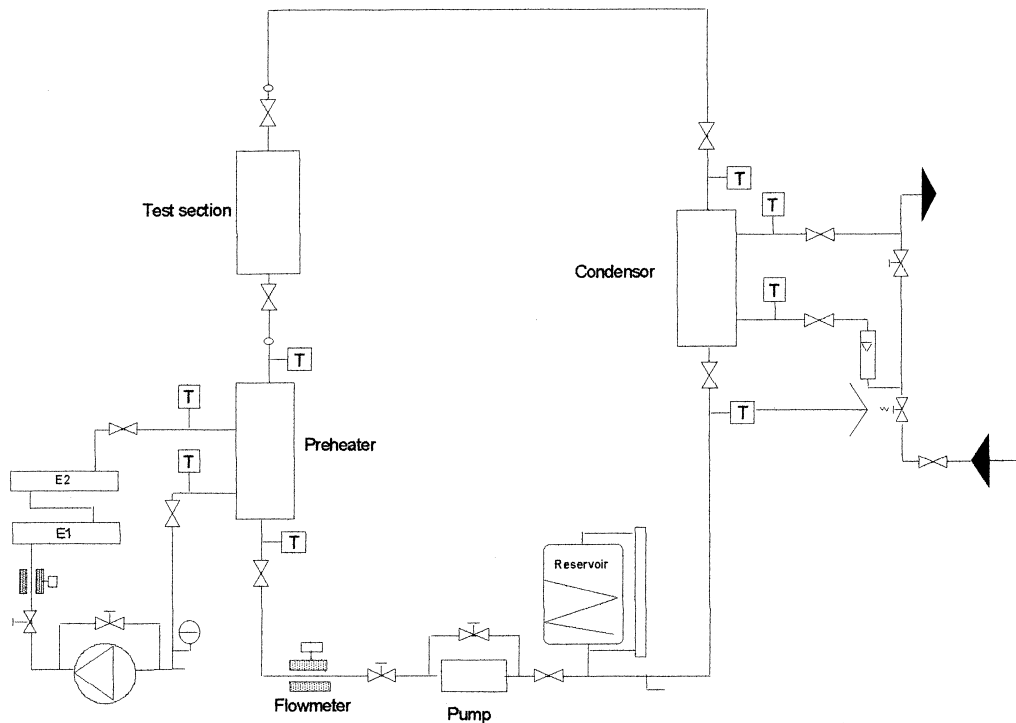


Fig. 1. Experimental apparatus.

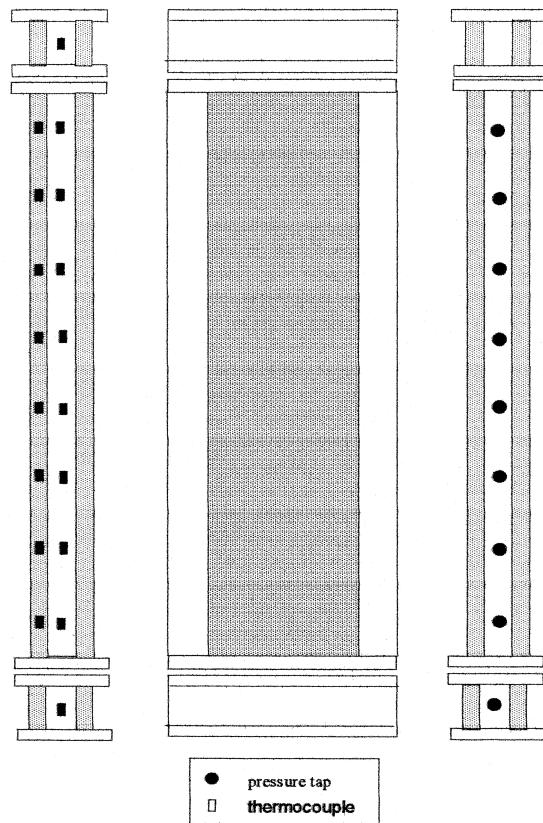


Fig. 2. Test section.

Moreover, this temperature provides a better understanding of the phenomena occurring in the channel. For example, nucleation departure or a possible dry-out region can be detected from the wall temperature.

With these test conditions (the fluid entering the test section is already two-phase) the fluid temperature should not deviate far from the saturated temperature. But the pressure drop in the channel is large enough to modify the evolution of the fluid temperature. Eight additional thermocouples were also placed in the channel to detect this evolution.

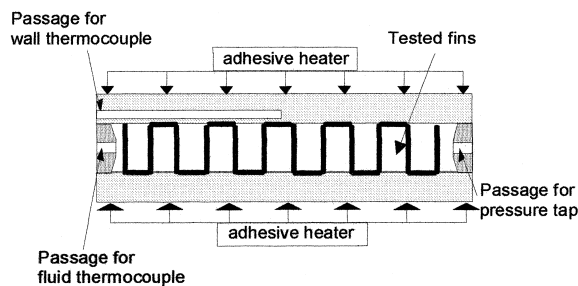


Fig. 3. Details of instrumentation.

Unfortunately, because of the random fin positions we cannot ensure that the thermocouples will only be in contact with the liquid (Fig. 3): they may touch a fin. To overcome this problem, we measure the absolute pressure at the inlet of the test section and the differential pressure along the length of the channel.

We can also determine the saturated pressure and thus the evolution of the saturated temperature.

3. Experimental procedure

All the heat transfer tests were carried out with an inlet test section two-phase flow. An experimental run was conducted as follows. The required flow rate and working pressure at the inlet to the test section were obtained by adjustment of the variable speed circulation pump and by heating the reservoir on the main circuit.

The hot water circuit heaters were controlled to adjust the inlet quality x_{in} to the test section. The inlet quality to the test section can also be determined from an energy balance on the preheater:

$$\dot{M}_{tp} C_{pl} (\Delta T)_l + x_{in} \dot{M}_{tp} h_{lg} = \dot{Q}_{hot\ water} \tag{1}$$

Using the inlet quality x_{in} determined from the above equation, the quality at each thermocouple location is obtained from an energy balance on the portion of the test section taken into account:

$$(x_{out} - x_{in}) \dot{M}_{tp} h_{lg} = \dot{Q}A \tag{2}$$

where A correspond to the area of the considered portion.

The electrical adhesive heaters were then applied and by continual adjustment of all three parameters, the required experimental conditions were attained at thermal equilibrium.

An axial profile of wall and bulk temperatures along the test section is drawn in Fig. 4 for a perforated fin geometry. Included on this plot is the local quality

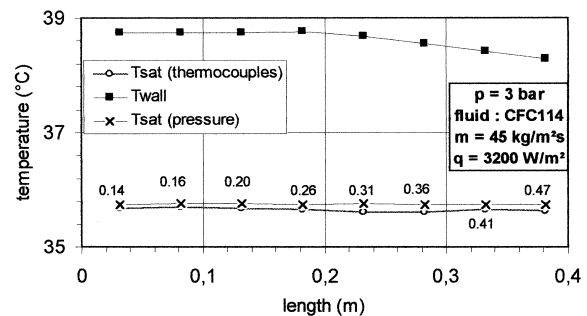


Fig. 4. Typical temperature profiles along perforated fin test section.

from the net heat input, the mass flux and the appropriate latent heat as explained before. The test conditions were set at a mass flux of 45 kg/m² s and a heat flux value of 3200 W/m².

Two kinds of measurement give us the fluid temperature as it has already been underlined, fluid thermocouples and pressure taps along the test section. As shown in Fig. 4 the fluid temperatures measured with the thermocouples are in accordance with those determined from the pressure measurement.

A slight decrease of fluid temperature is observed (about 0.4°C) between the inlet and outlet of the test section, due to the pressure drop along the channel.

A significant decrease is noted for the wall temperature for a 0.26 value of vapour quality. This observation will be interesting to analyse the heat transfer coefficient evolution.

The slight difference between the fluid and wall temperature (about 3°C) must be underlined. It also justifies paying particular attention to the experiments which are very difficult under these conditions.

With this plot it is then possible to derive the temperature difference between the wall and bulk and to obtain the local heat transfer coefficient (Fig. 5)

$$\alpha(z) = \frac{\dot{q}}{T_w(z) - T_{sat}} \quad (3)$$

An abrupt change in the slope is observed in Fig. 5. The heat transfer coefficient seems to be constant until the 0.26 vapour quality value is reached. As we have already explained, this evolution is linked to the wall temperature evolution.

Once again, we can see how important the local instrumentation is. With a global measurement, the change in the slope would not have been detected.

4. Remarks on measurement accuracy

The evaluation of the accuracy in the determination

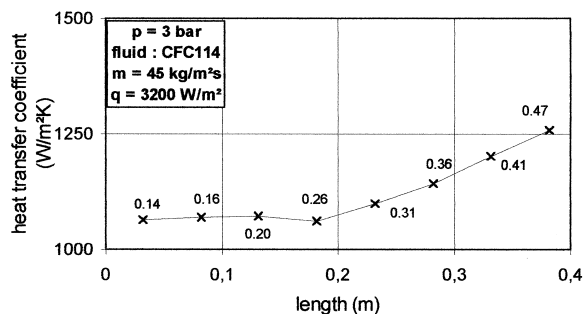


Fig. 5. Heat transfer coefficient along perforated fin test section.

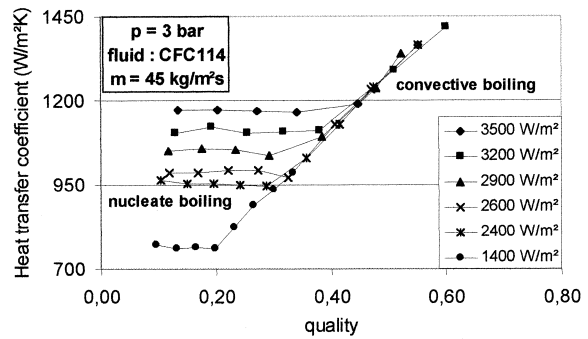


Fig. 6. Heat transfer coefficient versus quality.

of the local heat transfer coefficient gives a relative error of 15% for the more difficult conditions characterised by a low temperature difference between the wall and the saturated fluid (about 2°C). The evaluation of inlet vapour quality presents a relative error of 15%. Moreover, preliminary tests confirm the stability and repeatability of data with increasing or decreasing heat flux.

5. Analysis of the results: influence of quality, heat flux and mass flux

The measured variations of the two-phase flow heat transfer coefficient with quality, mass flux and heat flux for flow boiling of CFC114 in the different types of fins are presented here. A plot of the boiling heat transfer coefficients against quality, with heat flux as a parameter, is presented in Fig. 6 for a mass flux of 45 kg/m² s in a perforated fin geometry.

This figure suggests that the heat transfer phenomenon can be divided into two regions: a nucleate boiling region where the heat transfer coefficients depend on the heat flux but are independent of the vapour quality, and a convective boiling region where the heat transfer coefficient is independent of the heat flux.

This is also demonstrated in Fig. 7 where the heat transfer coefficient versus heat flux, with the quality as a parameter, is shown. For high quality values (x = 40%), the lines for the heat transfer coefficients are horizontal, i.e., independent of heat flux until the heat flux reaches the maximum test value. For low quality values (x = 20%), the heat transfer coefficient rises with the heat flux.

The influence of the mass flux is presented in Fig. 8. In the region where nucleate boiling is dominant, the heat transfer coefficient is independent of mass flux while it is dependent on the mass flux in the convective boiling region.

Two kinds of boiling regimes have been observed in this perforated fin geometry: a nucleate boiling region

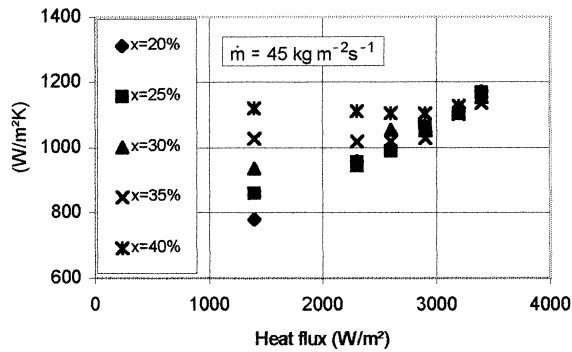


Fig. 7. Influence of heat flux.

for low vapour quality values, where the heat flux influences the heat transfer coefficient and a convective boiling region for high vapour quality values where the heat transfer coefficient is independent of the heat flux but is dependent on the mass flux and quality. Heat transfer increases with increasing mass flux and quality.

By direct viewing, we compared this thermal regime with the hydraulic regime. It was observed that for points obtained at low mass qualities and situated in the nucleate boiling area, the flow appeared to be bubbly or a slug flow regime. At higher qualities, the flow was annular in configuration, bubble nucleation on the heated surface appeared to be completely suppressed and the convective boiling regime was predominant.

In conclusion we can associate the nucleate boiling with a bubbly flow regime and the convective boiling regime with an annular flow regime.

6. Analysis of the results: influence of the fins dimensions

To examine the effect of channel geometry on the local heat transfer coefficient and on the two different

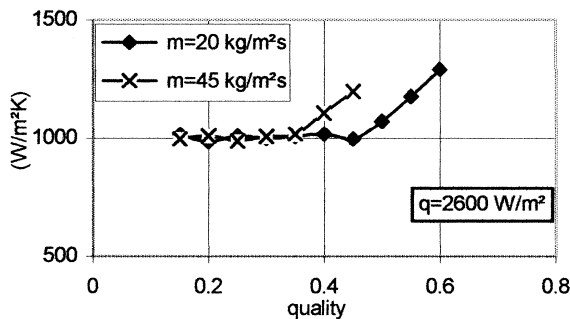


Fig. 8. Influence of mass flux.

boiling regimes, five different geometries were tested and are summarised in Table 1.

6.1. Influence of fin length

Tests were carried out using the same experimental conditions described earlier with two offset strip fins with different fin lengths (OSF01 — $L = 3.18$ mm and OSF02 — $L = 9.52$ mm). Fig. 9 shows the recorded results.

The trends in the data indicate that, for a given mass flux (here $45 \text{ kg/m}^2 \text{ s}$), the heat transfer coefficients for the two kinds of fin differ by about 35%. The results represented in Fig. 9 are sufficiently different to conclude that the overall two-phase heat transfer coefficient is very sensitive to changes in fin dimensions.

With the offset strip fin OSF02, whose fin is longer, the two boiling regimes can be observed. In the first region, for weak vapour quality values, the heat transfer coefficient depends on heat flux (nucleate boiling region) while in the second region, for high vapour quality values, the heat transfer coefficient depends only on quality and mass flux. Under the same experimental conditions with the offset strip fin OSF01, no nucleate boiling region is observed. All the data are independent of heat flux and viewing shows that the annular flow regime is predominant in the test section.

6.2. Influence of the fin height

The effect of the fin height was studied with two perforated fin geometries Perf01 and Perf02. These two geometries were similar except for the fin height. Fig. 10 shows the results obtained under the same experimental conditions with these two geometries.

Here again the trends in the data indicate that, for a given mass flux (here $45 \text{ kg/m}^2 \text{ s}$), the heat transfer coefficients for the two kinds of fin differ by about 30%. Once again, the two sets of results represented in

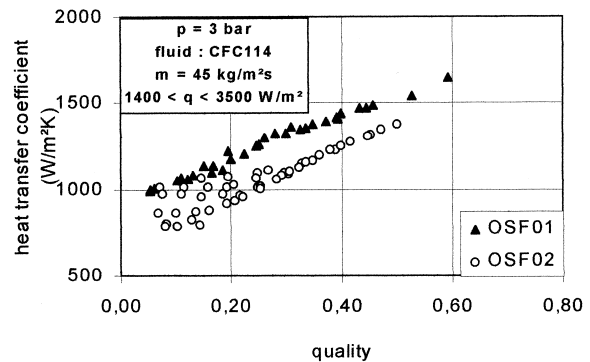


Fig. 9. Influence of fin length.

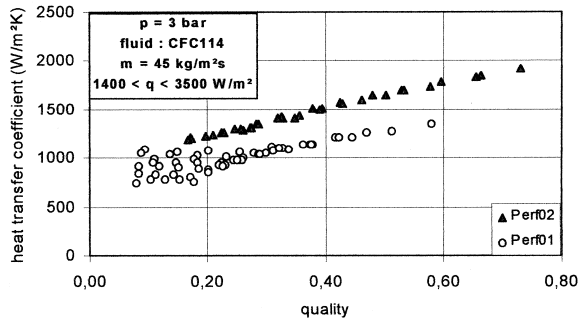


Fig. 10. Influence of fin height.

Fig. 10 are sufficiently different to conclude that the overall two-phase heat transfer coefficient is very sensitive to changes in fin dimensions.

With the perforated fin Perf01, whose fin is higher, the two boiling regimes can be observed. In this first region the heat transfer coefficient depends on the heat flux (nucleate boiling region) while in the second region the heat transfer coefficient only depends on the quality and mass flux. Using the same experimental conditions and the perforated fin Perf02, no nucleate boiling region is observed. All the data are dependent of heat flux and viewing shows that the annular flow regime is predominant in the test section.

6.3. Influence of fin density

The effect of the fin density was studied with two perforated fin geometries Perf01 and Perf03. These two geometries were similar except for the fin density. Fig. 11 shows the results obtained under the same experimental conditions with these two geometries.

The trends in the data indicate that, for a given

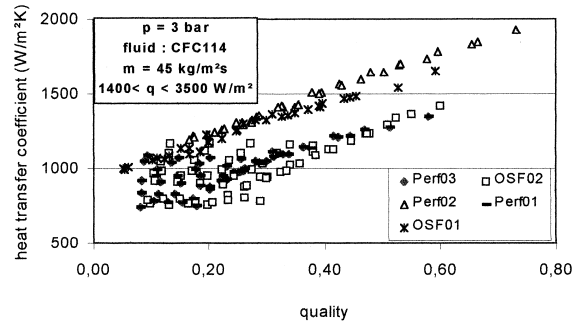


Fig. 12. Heat transfer coefficient versus quality.

mass flux (here 45 kg/m² s) the heat transfer coefficients for the two kinds of fin do not differ. The overall two-phase heat transfer coefficient is not very sensitive to changes in fin density.

Whatever the perforated fin (Perf01 or Perf03), the two boiling regimes can be observed. In the first region the heat transfer coefficient depends on the heat flux (nucleate boiling region) while in the second region the heat transfer coefficient only depends on the quality and mass flux.

7. Results analysis

The convective boiling regime is generally the dominant heat transfer mechanism for OSF fins with a small fin length or for perforated fins with a small fin height. For those fin geometries, the convective regime appears not only for the medium and high vapour quality but also at the lowest values of vapour quality. These observations shown in Fig. 12 can be easily explained: on the short length, a laminar boundary

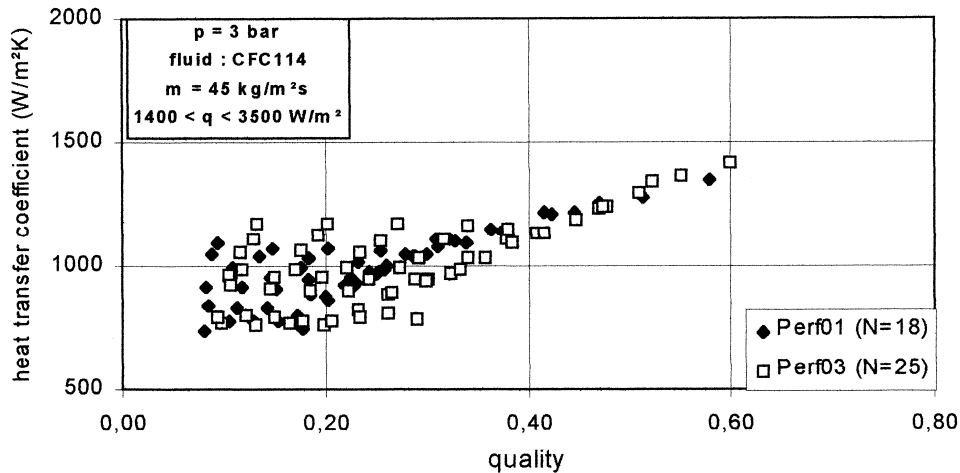


Fig. 11. Influence of fin density.

Table 2
Comparison between experimental results and correlations (percent of data predicted with $\pm 35\%$)

	Chen [11]	Carey [5]	Liu and Winterton [12]	Wadekar [13]	Steiner and Taborek [14]
Dent01	74	78	49	0	30
Dent02	71	99	57	0	25
Perf01	96	69	98	0	15
Perf02	96	80	39	0	35
Perf03	99	57	87	0	40

layer in the liquid phase is developed, followed by its destruction in the wake region between strips. Greater enhancement is obtained by using a shorter strip length.

The boiling regime becomes the dominant heat transfer mechanism with sufficiently high wall superheat. This wall superheat may be increased with the heat flux: in fact nucleate boiling appears with the highest values of heat flux. High wall superheat may also be obtained with a low convective heat transfer coefficient: low vapour quality or mass velocity involve a low convective heat transfer coefficient and promote a nucleate boiling regime. For the same reasons, fin geometries with high fin length which reduce the convective effects generally show a dominant nucleate boiling regime.

8. Construction of a semi-empirical model

In flow boiling, the nucleate and convective components are superimposed by a very complex mechanism. Three main models exist in the present literature [10], the superposition model using the addition of two components with a suppression factor, the enhancement model and the asymptotic model based on an asymptotic addition of two boiling components.

As will be explained, we propose to use an asymptotic model

$$\alpha^n = \alpha_{cv}^n + \alpha_{nb}^n \quad (4)$$

which assures a smooth transition as the boiling mechanism changes from nucleate (nb) to convective (cv). The case $n = 1$ represents the superposition model and $n \rightarrow \infty$ is the case for which the larger of the two mechanisms is predominant.

8.1. Treatment of convective boiling effect

A substantial fraction of the heat transfer measurements obtained in this study corresponded to flow conditions in which annular film flow evaporation was the dominant heat transfer mechanism. We will examine

different methods of correlating the convective boiling component α_{cv} .

The convective boiling heat transfer coefficient is very often expressed by

$$\alpha_{cv} = F\alpha_l \quad (5)$$

where the ratio F is defined as the two-phase convection multiplier.

Several correlations have been proposed by authors to evaluate the F factor. Table 2 shows the results obtained using some well-known correlations for each test geometry.

The data seem to be well correlated in terms of a version of the F -parameter used by Chen [11] to correlate the forced convective effects for flow boiling in vertical tubes. Chen correlated the convective heat transfer data by using the F factor and the Lockhart–Martinelli parameter [15]. The F factor is defined as the ratio of the two-phase heat transfer coefficient to the single-phase liquid fraction heat transfer coefficient

$$F = \frac{\alpha}{\alpha_l} = 1 + 1.8X^{-0.79} \quad (6)$$

The term α_l is computed from the single phase correlation for the specific geometry. For the offset strip fin geometries, the Wieting correlation [16] is used, and for the perforated fin geometries the Shah correlation [17] is proposed.

The expression of the Martinelli parameter X

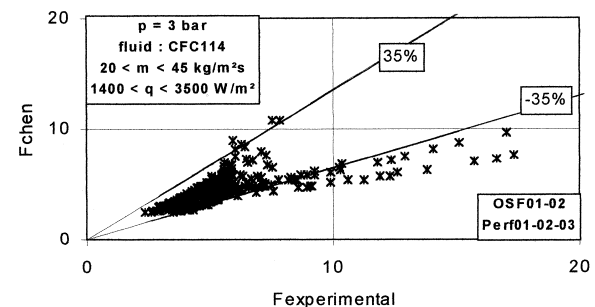


Fig. 13. Comparison between Chen correlation and experimental results.

depends on the nature of each phase and it can be written X_{lt} , X_{lv} , X_{ll} , or X_{ll} . The liquid and vapour friction factors were determined from the laminar or turbulent correlations proposed by Wieting or Shah.

In Fig. 13, a comparison between the experimental F -factor and the F -factor used by Chen is shown. Eighty-two percent of the data are predicted with $\pm 35\%$ with the Chen correlation. Only the experimental results obtained at a very low mass flux are not well predicted by the Chen correlation.

The discrepancy between experimental data and the calculated data with the Chen correlation may be easily explained by the following reasons. The Chen correlation has been initially developed for smooth tubes and the present work shows that the extrapolation of the method to complex and confined geometries (as OSF and perforated fins) involves a reduced quality of prediction.

The evaluation of a single-phase heat transfer coefficient and of the Lockhart Martinelli parameter is made with adequate correlation (Wieting correlation for the OSF fins, and Shah correlation for the perforated fins) which nevertheless may show some deviations with experimental data as can be seen in Table 3.

8.2. Treatment of the nucleate boiling effect

To correlate the nucleate boiling data, we propose to use the Cooper correlation [18] which can be expressed for pure CFC114 by:

$$\alpha_{npb} = 8.41 \dot{q}^{0.67} p_{red}^{0.12} (-\log_{10} p_{red})^{-0.55} \quad (7)$$

where the parameter p_{red} is defined as the ratio of the saturated pressure and the reduced pressure of the fluid. This parameter is frequently introduced in the nucleate boiling correlations based on the corresponding state method [18,19]. The constant 8.41 has been evaluated from the analysis of experimental data on CFC114 nucleate boiling.

The comparison between the experimental nucleate boiling heat transfer coefficients and the nucleate pool boiling heat transfer coefficients obtained with the Cooper correlation is shown in Fig. 14.

With the correlation, 95% of the nucleate boiling data are predicted within $\pm 35\%$. As it was earlier

Table 3
Comparison between experimental results and correlations (liquid phase) (Wieting and Shah correlations)

Type of fin	OSF01	OSF02	Perf01	Perf02	Perf03
Mean deviation (%)	11	18	39	38	27

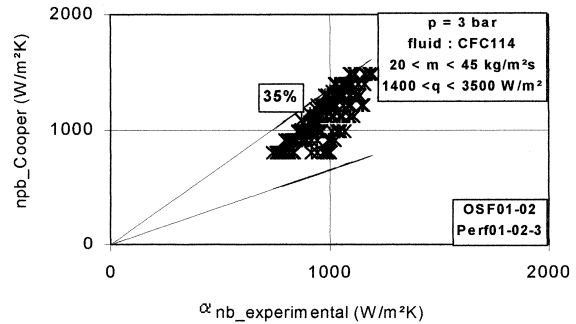


Fig. 14. Comparison between Cooper correlation and experimental results.

emphasised two different mechanisms have been clearly identified: a nucleate boiling regime (for low vapour quality values) and a convective boiling regime (for high vapour quality values). Moreover, an abrupt transition from nucleate to convective boiling has been detected. It corresponds to the case $n \rightarrow \infty$ in the asymptotic model. To use this form of the asymptotic model, both the nucleate pool boiling term α_{npb} with the Cooper correlation and the convective term $F\alpha_l$ with the Chen factor would be calculated, and the greater of the two values would be taken into consideration.

Fig. 15 shows the comparison between the experimental heat transfer coefficient and the semi-empirical heat transfer coefficient. With the asymptotic model, the data are, for the main part, predicted with $\pm 35\%$.

9. Conclusions

This study enabled local measurement of the heat transfer coefficient in compact heat exchangers to be obtained. Two kinds of boiling regimes have been detected.

On the one hand, there is the nucleate boiling regime where the heat transfer coefficient depends on heat flux but is independent of quality and mass flux. Only the

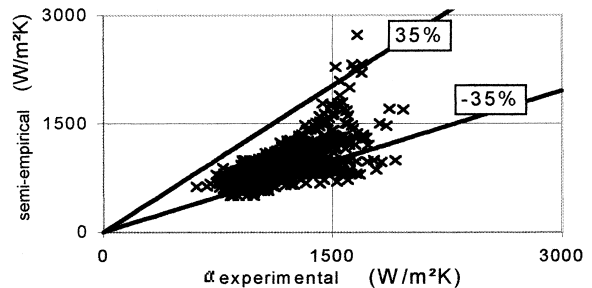


Fig. 15. Comparison between experimental results and semi-empirical model.

data obtained at low quality values are concerned by the nucleate boiling. On the other hand, the convective boiling depends on quality and mass flux but is completely independent of heat flux. Only the data obtained at high quality values are concerned by this mechanism.

The influence of the fin dimension emphasised the effect of fin length, height and density on the boiling regime. It appeared clearly that the decrease of fin height or length suppresses the nucleate boiling regime. The influence of fin density is not so evident in the boiling regime.

To help the manufacturers to design this kind of heat exchanger, a semi-empirical model, based on the asymptotic model is proposed in this paper. It allows prediction of the heat transfer coefficient regardless of the boiling regime, within $\pm 35\%$.

References

- [1] J.M. Robertson, Boiling heat transfer with liquid nitrogen in brazed-aluminium plate–fin heat exchangers, 1979, pp. 151–164.
- [2] J.M. Robertson, P.C. Lovegrove, Boiling heat transfer with Freon 11 in brazed aluminium plate–fin heat exchangers, *Journal of Heat Transfer* 105 (1983).
- [3] J.M. Robertson, The correlation of boiling coefficients in plate–fin heat exchanger passages with a film flow model, in: 7th International Heat Transfer Conference, Munich, 1982, pp. 341–345.
- [4] J.M. Robertson, The prediction of convective boiling coefficients in serrated plate–fin passages using an interrupted liquid-film flow model, *ASME HTD* 34 (1984) 163–171.
- [5] V.P. Carey, G.D. Mandrusiak, Annular film-flow boiling of liquids in a partially heated vertical channel with offset strip fins, *International Journal of Heat and Mass Transfer* 29 (6) (1999) 927–939.
- [6] G.D. Mandrusiak, V.P. Carey, Convective boiling in vertical channels with different offset strip fin geometries, *Transactions of ASME* 111 (1989) 156–165.
- [7] E. Michallon, Etude du comportement de l'écoulement dans des canaux de section rectangulaire constitués de plaques et d'ailettes brasées. Thèse de l'Université de Nancy I, novembre, 1993.
- [8] A. Feldman, C. Marvillet, M. Lebouché, An experimental study of boiling in plate fin heat exchangers, 2nd European Thermal-Sciences and 14th UIT National Heat Transfer Conference 1 (1996) 445–450.
- [9] A. Feldman, L. Margat, C. Marvillet, B. Thonon, Transition from nucleate boiling to convective boiling in compact heat exchangers. Pool Boiling Conference, Eurotherm Seminar No. 47, Paderborn, Germany, 1996.
- [10] R.L. Webb, N.S. Gupte, A critical review of correlations for convective vaporization in tubes and tube banks, *Heat Transfer Engineering* 13 (3) (1992).
- [11] J.C. Chen, Correlation for boiling heat transfer to saturated fluids in convective flow, *I&EC Process Design and Development* 5 (3) (1966) July.
- [12] Z. Liu, R.H.S. Winterton, A general correlation for saturated and subcooled flow boiling in tubes and annuli, based on a nucleate pool boiling equation, *International Journal of Heat Transfer* 34 (11) (1991) 2759–2766.
- [13] V.V. Wadekar, Flow boiling — a simple correlation for convective heat transfer component, *Proceedings of the Ninth International Heat Transfer Conference, Jerusalem* 2 (1990) 87–91.
- [14] D. Steiner, J. Taborek, Flow boiling heat transfer in vertical tubes correlated by an asymptotic model, *Heat Transfer Engineering* 13 (2) (1992).
- [15] R.W. Lockhart, R.C. Martinelli, Proposed correlation of data for isothermal two phase, two component flow in pipes, *Chemical Engineering Progress* 45 (1) (1949) January.
- [16] A.R. Wieting, Empirical correlations for heat transfer and flow friction characteristics of rectangular offset fin plate fin heat exchangers. *Transactions of ASME, Journal of Heat Transfer*, August, 1975.
- [17] R.K. Shak, A.L. London, *Laminar Flow Forced Convection in Ducts*, Academic Press, 1978.
- [18] M.G. Cooper, Flow boiling — the 'apparently nucleate' regime, *International Journal of Heat and Mass Transfer* 32 (3) (1989) 459–464.
- [19] D. Gorenflo, *VDI Heat Atlas Section HA*, VDI Verlag Düsseldorf, 1993.